# The stepwise formation of mixed-metal coordination networks using complexes of 3-cyanoacetylacetonate

**Andrew D. Burrows,*[a] Kevin Cassar,[a] Mary F. Mahon*[a] and John E. Warren[b]**

***Received 9th February 2007, Accepted 4th April 2007***
***First published as an Advance Article on the web 23rd April 2007***
**DOI: 10.1039/b702074k**



The complexes $[Cu(L^1)_2]$ **1**, $[Fe(L^1)_3]$ **3** and $[Al(L^1)_3]$ **4** [$L^1 = CH_3C(O)C(CN)C(O)CH_3$] have been prepared for use as metallo-ligands in mixed-metal coordination networks. Surprisingly, the nature of the copper precursor is important in the synthesis of **1**, with the reaction between $Cu(NO_3)_2{\cdot}3H_2O$, $HL^1$ and $NEt_3$ giving $[Cu_6(\mu_3\text{-}OMe)_4(\mu\text{-}OMe)_2(L^1)_6]$ **2** instead of the anticipated **1**, which was obtained with $CuCl_2{\cdot}2H_2O$ under the same conditions. Compound **1** reacts with $AgNO_3$ to form $[Cu(L^1)_2{\cdot}AgNO_3]_\infty$ **5**, the structure of which contains one-dimensional chains in which $Ag^+$ ions bridge between molecules of **1**. These chains are cross-linked into ladders by bridging nitrates. The product obtained from the reaction of **3** and $AgNO_3$ is crucially dependent on the solvent used. The reaction in methanol–acetone gives $[Fe(L^1)_3{\cdot}AgNO_3]_\infty$ **6**, $\{[Fe_2(\mu\text{-}OMe)_2(L^1)_4{\cdot}2AgNO_3]{\cdot}CH_3C(O)CH_3\}_\infty$ **7** and $[Fe_2(\mu\text{-}OMe)_2(L^1)_4{\cdot}AgNO_3]_\infty$ **8**. Compounds **6** and **8** both have one-dimensional chain structures, whereas **7** has a two-dimensional layer structure. The reaction in methanol gives **6** and **8** as the major products and, in addition, small quantities of $\{[AgFe_2(\mu\text{-}OMe)_2(L^1)_4]OH{\cdot}0.4H_2O\}_\infty$ **9**. Compound **9** has a three-dimensional structure based on doubly interpenetrated PtS nets. Compounds **7–9** contain $Fe_2(\mu\text{-}OMe)_2(L^1)_4$ dimers, but the coordination properties of the dimers differ, with all the cyanides coordinated in **7** and **9** but one uncoordinated in **8**. The orientation of the cyanide groups depends on the relative chirality of the iron centres. A transmetallation reaction occurs between **4** and $AgNO_3$ to give $[Ag(L^1)]_\infty$ **10**, which has a two-dimensional layer structure. Compounds **2**, **3** and **5–10** have been characterised by X-ray crystallography.

## Introduction

Over recent years there has been a remarkable upsurge of interest in coordination networks.[1] These materials, also known as metal–organic frameworks, are formed when ligands bridge between metal centres or small clusters (secondary building units, SBUs). Much of the interest with these structures has arisen because some of them are able to retain their structures and crystallinity on removal of solvents, and this enables the materials to display interesting porosity properties.[2] Potential applications in hydrogen storage[3] are especially topical and have received considerable attention, but coordination networks are also attractive for a range of other applications[4] including separations,[5] catalysis,[6] sensing[7] and waste water treatment.[8]

Most synthetic routes to coordination networks employ self-assembly, and use the direct reaction between metal ions or pre-formed SBUs and linking ligands to form the network structure. Sometimes a base is added to generate the ligand *in situ*, for example in the case of polycarboxylates generated from the acids. While simple, these approaches can be difficult to control, and the synthesis of a specific coordination network may be crucially dependent on the reaction conditions.[9] For example, we recently showed that the quality of the DEF (diethylformamide) solvent was a key factor in determining whether $[Zn_4(\mu_4\text{-}O)(\mu\text{-bdc})_3]_\infty$ (MOF-5, bdc = 1,4-benzenedicarboxylate) was formed from the reaction of $Zn(NO_3)_2{\cdot}6H_2O$ and $H_2bdc$.[10] When hydrolysis of the solvent had occurred, this led to the formation of $NEt_2H_2^+$ cations, which templated the formation of an anionic network.

The self-assembly approach is also of limited use in forming mixed-metal networks, in which two types of metal ion may have different structural and/or functional roles. With this in mind, we have sought to employ a stepwise approach to mixed-metal coordination networks. This involves reaction of a metal centre with a bifunctional ligand to give an isolable intermediate complex which itself can act as a building block in network formation.[11] The reaction of this metallo-ligand with a second metal centre can then be used to form the mixed-metal coordination network. The stepwise approach to coordination networks has previously been carried out using sulfonated dipyridine-*N*,*N*′-dioxide[12] and cyano-functionalised dipyrrinato ligands.[13]

Bifunctional ligands based on acetylacetonates are attractive for use in construction of mixed-metal networks. The chelating nature of the bidentate *O*,*O*-donor ensures relatively low lability, and the negative charge on the ligand allows access to neutral complexes. Acetylacetonates can be functionalised in several positions, though the symmetric ligands generated by 3-substitution and 1,5-disubstitution are most attractive for the formation of ordered structures.[14]

3-(4-Pyridyl)acetylacetonate has been used previously to form coordination networks,[15,16] but use of this ligand is limited by its tendency to decompose *via* a reverse-Claisen condensation.[17] In this paper we report the use of 3-cyanoacetylacetonate ($L^1$) as a

[a]*Department of Chemistry, University of Bath, Claverton Down, Bath, UK BA2 7AY. E-mail: a.d.burrows@bath.ac.uk, m.f.mahon@bath.ac.uk*
[b]*CLRC Daresbury Laboratory, Daresbury, Warrington, UK WA4 4AD*

bifunctional ligand. 3-Cyanoacetylacetone ($HL^1$) exists exclusively in the enol form, supported by an intramolecular O–H · · · O hydrogen bond.[18] Copper and cobalt network structures containing $L^1$ have been prepared,[19,20] but mixed-metal coordination networks based on $L^1$ are as yet unknown. In this paper we explore the synthesis of mixed-metal networks based on $L^1$ *via* the initial formation of copper(II), iron(III) and aluminium(III) complexes.

## Results

### Copper $L^1$ complexes

$[Cu(L^1)_2]$ **1** was prepared from the reaction between $CuCl_2{\cdot}2H_2O$ and $HL^1$ in methanol, in the presence of $NEt_3$. Microanalysis and IR spectroscopy confirmed the identity of the product, and the X-ray powder diffraction pattern verified that the structure was the same as that previously reported.[20] When $Cu(NO_3)_2{\cdot}3H_2O$ was used instead of $CuCl_2{\cdot}2H_2O$, a different product was obtained. The crystals formed were paler in colour and single crystal X-ray crystallography revealed that the compound was $[Cu_6(\mu_3\text{-}OMe)_4(\mu\text{-}OMe)_2(L^1)_6]$ **2**.

The asymmetric unit of **2** contains three crystallographically distinct copper centres, three $L^1$ ligands and three methoxy ligands. An inversion centre connects these into hexacopper complexes as shown in Fig. 1. These complexes can be thought of as comprising three $Cu_2(\mu\text{-}OMe)_2(L^1)_2$ dimers that are interlinked through $\mu_3$-methoxy groups.

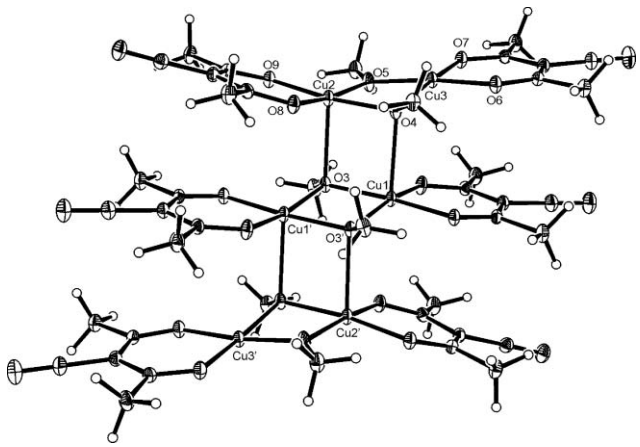


**Fig. 1** The molecular structure of $[Cu_6(\mu_3\text{-}OMe)_4(\mu\text{-}OMe)_2(L^1)_6]$ **2**. The primed atoms are related to unprimed atoms by the symmetry operation $1 - x$, $1 - y$, $1 - z$. Thermal ellipsoids are shown at the 30% probability level.

Two of the independent copper atoms, Cu(1) and Cu(2), have square pyramidal geometries while the third, Cu(3), has a square planar geometry. Both Cu(1) and Cu(2) are coordinated to two oxygen atoms from a $L^1$ ligand and three methoxy ligands, though for Cu(1) the methoxy ligands all have $\mu_3$-coordination whereas for Cu(2) one of them bridges between only two copper centres. Cu(3) is coordinated to two oxygen atoms from a $L^1$ ligand, one $\mu_2$-methoxy ligand and one $\mu_3$-methoxy ligand. Selected bond lengths and angles for **2** are given in Table 1. A comparison of the Cu–O bond lengths for the square pyramidal centres reveals that the bonds to the axial oxygen atoms [Cu(1)–O(4) and Cu(2)–O(3)] are longer than those to the equatorial oxygen atoms. This also reflects the unsymmetrical nature of the $\mu_3$-bridging mode in this compound, with the oxygen atoms each forming two short and one long Cu–O contact.

**Table 1** Selected bond lengths (Å) and angles (°) in the structure of $[Cu_6(\mu_3\text{-}OMe)_4(\mu\text{-}OMe)_2(L^1)_6]$ **2**[a]

| | | | |
|---|---|---|---|
| Cu(1)–O(1) | 1.9232(15) | Cu(2)–O(5) | 1.9042(16) |
| Cu(1)–O(2) | 1.9269(16) | Cu(2)–O(8) | 1.9325(16) |
| Cu(1)–O(3) | 1.9394(15) | Cu(2)–O(9) | 1.9235(16) |
| Cu(1)–O(4) | 2.4178(17) | Cu(3)–O(4) | 1.9472(16) |
| Cu(1)–O(3)′ | 1.9453(16) | Cu(3)–O(5) | 1.8973(16) |
| Cu(2)–O(3) | 2.3916(17) | Cu(3)–O(6) | 1.9173(16) |
| Cu(2)–O(4) | 1.9567(15) | Cu(3)–O(7) | 1.9146(17) |
| O(1)–Cu(1)–O(2) | 92.53(7) | O(7)–Cu(3)–O(6) | 92.42(7) |
| O(3)–Cu(1)–O(3)′ | 79.88(7) | O(5)–Cu(3)–O(4) | 78.95(7) |
| Cu(1)–O(3)–Cu(1)′ | 100.12(7) | Cu(3)–O(4)–Cu(2) | 98.29(7) |
| O(9)–Cu(2)–O(8) | 91.66(7) | Cu(3)–O(5)–Cu(2) | 101.93(8) |
| O(5)–Cu(2)–O(4) | 78.55(7) | | |

[a] Primed atoms generated by the symmetry operation $-x + 1$, $-y + 1$, $-z + 1$.

The two outer $Cu_2(\mu\text{-}OMe)_2(L^1)_2$ dimers in the hexacopper complex are markedly curved, with the $L^1$ ligands bent away from the central $Cu_2(\mu\text{-}OMe)_2$ unit. The angle between the equatorial coordination planes of Cu(2) and Cu(3) is 159°. Long range interactions between cyanide groups and the square planar copper centre link the hexacopper complexes into tapes [Cu(3) · · · N(3) 2.666(2) Å], though the C–N–Cu angle (127°) is considerably distorted from linearity. A similar, though shorter, interaction was observed in the crystal structure of **1** [Cu · · · N 2.468(3) Å, C–N–Cu 116°].[20]

### Iron $L^1$ complexes

$[Fe(L^1)_3]$ **3** was synthesised from the reaction between $Fe(NO_3)_3{\cdot}9H_2O$ and three equivalents of $HL^1$ in methanol, in the presence of $NEt_3$. Although relatively low-yielding, vapour diffusion of the base into a solution of $Fe(NO_3)_3{\cdot}9H_2O$ and $HL^1$ allows for the formation of a pure, crystalline product after 2 h. When the reaction mixture is left for longer times, a higher return of material is given, but X-ray powder diffraction studies indicated this to include another as yet unidentified product.

Compound **3** was characterised on the basis of microanalysis and IR spectroscopy, and its identity was confirmed by a single crystal X-ray analysis. The crystal structure revealed the presence of two molecules of **3** in the asymmetric unit. Both iron centres adopt a distorted octahedral geometry, and one of the independent molecules in shown in Fig. 2a.

Selected bond lengths and bond angles for **3** are given in Table 2.

There are no chemically significant differences in the bond lengths and bond angles between the two independent molecules. The Fe–O distances range from 1.981(2) to 1.995(2) Å and from 1.980(2) to 1.995(2) Å for the molecules based on Fe(1) and Fe(2) respectively. The $L^1$ ligand bite angles vary from 85.41(9) to 86.75(9)° in the molecule based on Fe(1) and from 84.98(8) to 86.71(9)° in the molecule based on Fe(2).

The $FeO_2C_3$ chelate rings are generally non-planar, with the iron atoms sitting out of the plane defined by the ligand atoms in the ring. This distortion can be quantified by the angle between the $FeO_2$ plane and the $O_2C_3$ plane defined by the ligand atoms in the chelate ring. These inter-plane angles are 2°, 3° and 17°

 

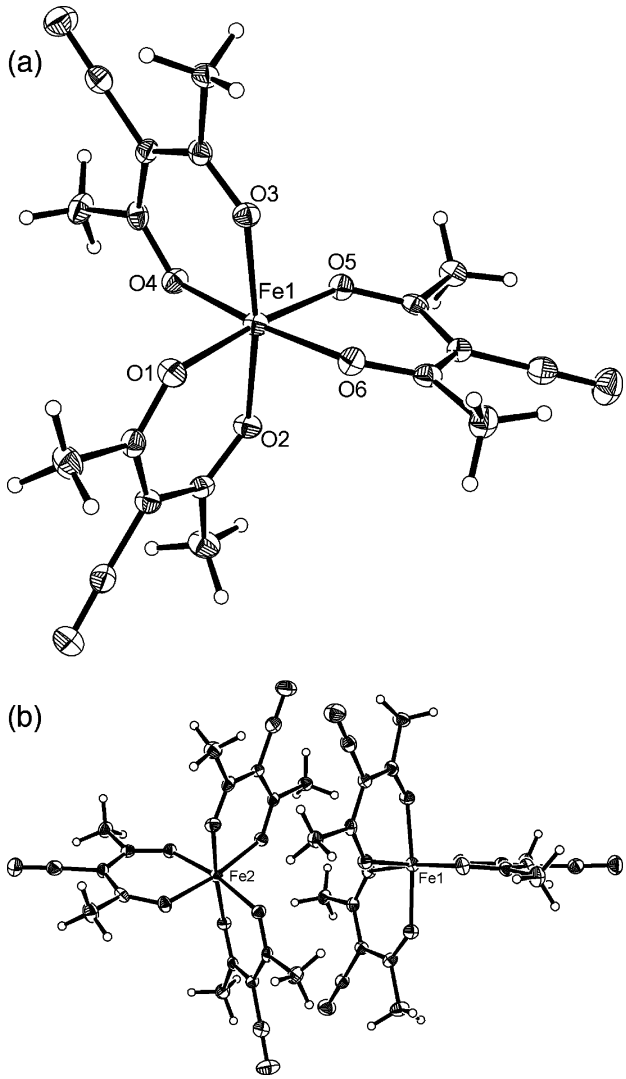


**Fig. 2** (a) The molecular structure of one of the independent molecules in the crystal structure of $[Fe(L^1)_6]$ **3**. Thermal ellipsoids are shown at the 30% probability level. (b) The pairwise interaction between the two independent molecules of **3**.

**Table 2** Selected bond lengths (Å) and angles (°) in the structure of $[Fe(L^1)_3]$ **3**

| | | | |
|---|---|---|---|
| Fe(1)–O(1) | 1.986(2) | Fe(2)–O(7) | 1.994(2) |
| Fe(1)–O(2) | 1.987(2) | Fe(2)–O(8) | 1.989(2) |
| Fe(1)–O(3) | 1.981(2) | Fe(2)–O(9) | 1.995(2) |
| Fe(1)–O(4) | 1.995(2) | Fe(2)–O(10) | 1.990(2) |
| Fe(1)–O(5) | 1.995(2) | Fe(2)–O(11) | 1.989(2) |
| Fe(1)–O(6) | 1.994(2) | Fe(2)–O(12) | 1.980(2) |
| O(1)–Fe(1)–O(2) | 86.75(9) | O(8)–Fe(2)–O(7) | 84.98(8) |
| O(3)–Fe(1)–O(4) | 86.64(9) | O(10)–Fe(2)–O(9) | 86.71(9) |
| O(6)–Fe(1)–O(5) | 85.41(9) | O(12)–Fe(2)–O(11) | 86.06(9) |
| O(3)–Fe(1)–O(2) | 171.29(9) | O(10)–Fe(2)–O(7) | 170.05(9) |
| O(1)–Fe(1)–O(5) | 174.60(9) | O(11)–Fe(2)–O(8) | 175.38(9) |
| O(6)–Fe(1)–O(4) | 173.29(9) | O(12)–Fe(2)–O(9) | 171.11(9) |

for the three ligands in the molecule containing Fe(1) and 9°, 11° and 23° for the ligands in the molecule containing Fe(2). Together with the distortions from regular octahedral coordination, this has a significant impact on the relative orientations of the cyanide groups. For a perfect octahedral complex, the cyanide groups would be expected to be oriented at 120° to each other, in a similar manner to 1,3,5-tricyanobenzene. For **3**, the angles between the cyanide groups are 107°, 108° and 144° for the molecule containing Fe(1), and 111°, 117° and 131° for the molecule containing Fe(2). These deviations from 120° are important as they will influence the structure of the networks formed when the cyanide groups coordinate to a second metal.

Similar deviations have been seen for complexes derived from 3-(4-pyridyl)-2,4-pentanedione ($HL^2$), and network structures based on $Al(L^2)_3$ and $Fe(L^2)_3$ do not form honeycomb structures as would have been expected with 120° angles.[16] In this case the deviations from 120° angles between the pyridyl groups were attributed to the presence of the aromatic group, and believed to derive from minimising the molecular volume. Aromatic groups are not present in **3**, and the wide angles observed in this structure occur together with a pairwise interaction between the two independent molecules. Thus a molecule containing Fe(1) and a molecule containing Fe(2) interdigitate leading to a Fe···Fe separation of 5.84 Å (Fig. 2b).

### Aluminium $L^1$ complexes

When $Al(NO_3)_3{\cdot}9H_2O$ was reacted with $HL^1$ in the presence of $NEt_3$, the reaction did not give any product in high yield, so a different method was employed to form $[Al(L^1)_3]$ **4**. $Al(NO_3)_3{\cdot}9H_2O$ and $HL^1$ were dissolved in a 1 : 1 mixture of methanol and water to which $NaHCO_3$ in the same solvent mixture was added slowly with continuous stirring. A colourless powder precipitated after the complete addition of the base. This was separated by filtration and washed with water to remove unreacted base. The product was dried in air, and characterised as the hexahydrate by microanalysis. NMR spectroscopy confirmed the presence of the $[L^1]^-$ ligands and the solvate water molecules. Mass spectrometry provided further evidence for the formation of **4**, with significant ions observed in the MALDI spectrum at $m/z$ 422 ($[M + Na]^+$), $m/z$ 275, ($[M - L^1 + H]^+$), and $m/z$ 159, ($[M - 2L^1]^+$) [$M = Al(L^1)_3$].

### Synthesis of mixed metal networks

Compounds **1–4** were reacted with silver(I) salts to form mixed metal coordination networks. Silver(I) was chosen as the source of the linking metal due to its coordination flexibility, and its ready coordination to nitriles. Compound **2** is insoluble in most solvents, and only sparingly soluble in DMF. All attempts to form mixed metal networks with **2** failed, and the starting materials were recovered unreacted. A range of silver salts were used in reactions with **1–4**, and only the nitrate yielded compounds suitable for X-ray single crystal analysis.

**Copper–silver networks.** The reaction between $Cu(L^1)_2$ **1** and $AgNO_3$ in DMF–methanol gave blue crystals suitable for X-ray crystallography. The crystallographic analysis revealed the compound to be $[Cu(L^1)_2{\cdot}AgNO_3]_\infty$ **5**. The asymmetric unit of **5** consists of one copper centre, two $L^1$ ligands, one silver centre and one nitrate ion. The copper atom adopts a distorted square pyramidal geometry, with the equatorial positions occupied by four oxygen atoms from two different $L^1$ ligands. In this way, the coordination environment at copper observed in **1** is retained. The axial position in **5** is occupied by an oxygen atom from the nitrate

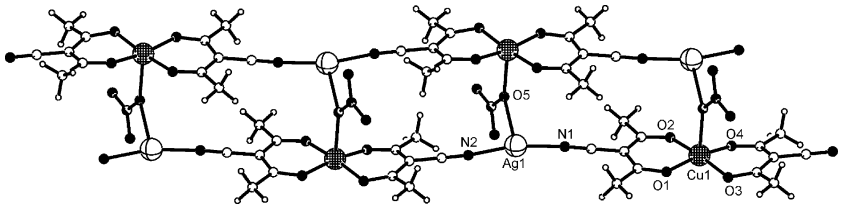


**Fig. 3** The ladder structure adopted in the crystal structure of $[Cu(L^1)_2{\cdot}AgNO_3]_\infty$ **5**.



ion. The silver ion adopts a distorted T-shaped geometry, being coordinated to two cyanide groups and also to the coordinated oxygen atom of the nitrate. Coordination to the two cyanide groups to silver(I) links the $Cu(L^1)_2$ complexes into one-dimensional polymeric chains. The bridging nitrate ligands interlink pairs of chains to form a ladder structure, as shown in Fig. 3.

Selected bond lengths and bond angles for **5** are given in Table 3. The equatorial Cu–O distances lie between 1.9264(10) and 1.9415(9) Å, with the bond to the nitrate longer, at 2.2229(12) Å. The $L^1$ ligand bite angles are 91.91(4)° and 92.19(4)°, within the range of those observed for **2**. For the silver atom, the Ag–O distances average 0.35 Å longer than the Ag–N distances.

One of the independent C–N–Ag angles is close to linearity, while the other is slightly bent [161.43(12)°]. Together with the N–Ag–N angle, 161.76(5)°, this leads to the ladders propagating in a linear manner. These ladders stack alongside each other into layers in the gross structure, which are supported by C–H···O hydrogen bonds. Similar interactions are present linking the layers into a three-dimensional structure.

**Iron–silver networks.** The reaction between $[Fe(L^1)_3]$ **3** and $AgNO_3$ in acetone–methanol gave pale red crystals after 2 weeks and darker red crystals when the reaction mixture was left for longer periods. The darker red crystals were shown by an X-ray single crystal analysis and X-ray powder diffraction to be $[Fe(L^1)_3{\cdot}AgNO_3]_\infty$ **6**, whereas analyses on the pale red crystals revealed these to be a mixture of $\{[Fe_2(\mu\text{-}OMe)_2(L^1)_4{\cdot}2AgNO_3]{\cdot}CH_3C(O)CH_3\}_\infty$ **7** and $[Fe_2(\mu\text{-}OMe)_2(L^1)_4{\cdot}AgNO_3]_\infty$ **8**, with **7** the major product.

The asymmetric unit of $[Fe(L^1)_3{\cdot}AgNO_3]_\infty$ **6** consists of one iron atom, three $L^1$ ligands, one silver atom and one nitrate anion. Selected bond lengths and angles are given in Table 4. The iron centre adopts a distorted octahedral geometry with the coordination sphere containing six oxygen atoms from three $L^1$ ligands, as in the structure of **3**. The silver ion is coordinated to two cyanide groups and an oxygen atom from the nitrate ion. This enables the $AgNO_3$ units to bridge between $Fe(L^1)_3$ moieties and link the iron complexes into one-dimensional chains, as shown in Fig. 4. One of the three cyanide groups present on each $Fe(L^1)_3$ moiety is uncoordinated, and this prevents cross-linking of the chains into layers.

The Fe–O distances range from 1.9655(11) to 1.9998(11) Å, with the lower values marginally shorter than the equivalent distances in **3**. The $L^1$ ligand bite angles around the iron centre range from 86.04(4) to 87.00(4)°, broadly in line with the range observed in

**Table 3** Selected bond lengths (Å) and angles (°) in the structure of $[Cu(L^1)_2{\cdot}AgNO_3]_\infty$ **5**[a]

| | | | |
|---|---|---|---|
| Ag(1)–N(1)″ | 2.1366(12) | Cu(1)–O(2) | 1.9301(9) |
| Ag(1)–N(2)′ | 2.1185(12) | Cu(1)–O(3) | 1.9396(9) |
| Ag(1)–O(5) | 2.4802(13) | Cu(1)–O(4) | 1.9415(9) |
| Cu(1)–O(1) | 1.9264(10) | Cu(1)–O(5) | 2.2229(12) |
| N(2)′–Ag(1)–N(1)″ | 161.76(5) | O(4)–Cu(1)–O(5) | 87.85(5) |
| N(1)″–Ag(1)–O(5) | 94.40(5) | O(1)–Cu(1)–O(5) | 98.92(5) |
| N(2)′–Ag(1)–O(5) | 102.95(5) | O(3)–Cu(1)–O(5) | 98.33(5) |
| O(1)–Cu(1)–O(2) | 92.19(4) | C(6)–N(1)–Ag(1)″ | 161.43(12) |
| O(3)–Cu(1)–O(4) | 91.91(4) | C(12)–N(2)–Ag(1)′ | 176.19(12) |
| O(2)–Cu(1)–O(5) | 92.89(5) | | |

[a] Primed atoms generated by the symmetry operation $-x+1, -y+1, -z+1$. Double primed atoms generated by the symmetry operation $-x+1, -y, -z$.

**Table 4** Selected bond lengths (Å) and angles (°) in the structure of $[Fe(L^1)_3{\cdot}AgNO_3]_\infty$ **6**[a]

| | | | |
|---|---|---|---|
| Ag(1)–N(1) | 2.2998(18) | Fe(1)–O(3) | 1.9747(11) |
| Ag(1)–N(3)′ | 2.3523(15) | Fe(1)–O(4) | 1.9979(11) |
| Ag(1)–O(9) | 2.3320(17) | Fe(1)–O(5) | 1.9964(11) |
| Fe(1)–O(1) | 1.9655(11) | Fe(1)–O(6) | 1.9998(11) |
| Fe(1)–O(2) | 1.9892(11) | | |
| N(1)–Ag(1)–N(3)′ | 99.41(6) | O(1)–Fe(1)–O(4) | 174.47(5) |
| N(1)–Ag(1)–O(9) | 133.76(6) | O(2)–Fe(1)–O(5) | 172.52(5) |
| O(9)–Ag(1)–N(3)′ | 121.11(6) | O(3)–Fe(1)–O(6) | 171.66(5) |
| O(1)–Fe(1)–O(2) | 87.00(4) | C(6)–N(1)–Ag(1) | 139.44(18) |
| O(3)–Fe(1)–O(4) | 86.04(4) | C(18)–N(3)–Ag(1)″ | 130.52(13) |
| O(5)–Fe(1)–O(6) | 86.05(4) | | |

[a] Primed atoms generated by the symmetry operation $x-1, -y+1/2, z-1/2$. Double primed atoms generated by the symmetry operation $x+1, -y+1/2, -z+1/2$.

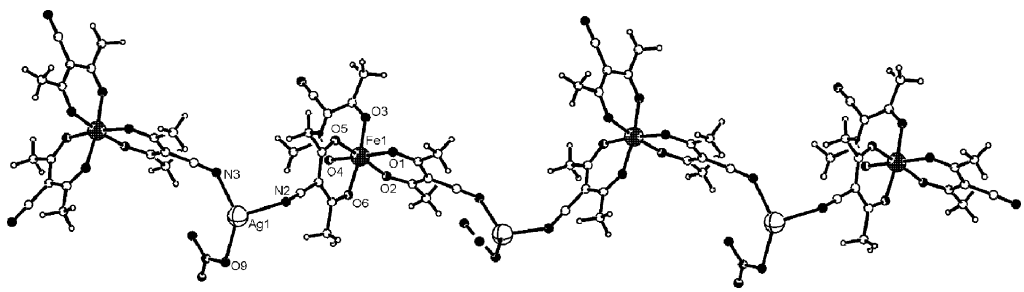


**Fig. 4** One of the chains in the crystal structure of $[Fe(L^1)_3{\cdot}AgNO_3]_\infty$ **6**.

 

**3**. The distortions of some of the chelate rings from planarity, observed in the structure of **3**, are also present in the structure of **6**. The angles between the $FeO_2$ plane and the $O_2C_3$ plane in the chelate ring are 4°, 6° and 19° for the three ligands. As with **3**, it is noticeable that one of these angles is considerably greater than the others. In **6**, the combination of these angles and distortions from a perfect octahedral metal geometry lead to changes in the relative orientations of the cyanide groups. For **6**, the angles between the cyanide groups are 114°, 115° and 131°, so the distortion in **6** is less than that in **3**.

The silver atom adopts a three-coordinate distorted trigonal planar geometry, with bond angles between 99.41(6)° and 133.76(6)°. The C–N–Ag angles are distorted from linearity, with C(6)–N(1)–Ag(1) 139.44(18)° and C(18)–N(3)–Ag(1)″ 130.52(13)°. This compares with the values of 161.43(12)° and 176.19(12)° observed for **5**. C–H···O hydrogen bonds involving oxygen atoms on the nitrate anions as acceptors reinforce each chain and interlink them into the gross structure.

The asymmetric unit of $\{[Fe_2(\mu\text{-}OMe)_2(L^1)_4{\cdot}2AgNO_3]{\cdot}CH_3C(O)CH_3\}_\infty$ **7** consists of two iron atoms, two methoxide ligands, four $L^1$ ligands, two silver centres, two nitrate anions and an included acetone molecule. Each iron centre is coordinated to two bidentate $L^1$ ligands and two methoxides giving a distorted octahedral geometry. The methoxides bridge between two iron centres, leading to the formation of $Fe_2(\mu\text{-}OMe)_2(L^1)_4$ dimers. The two independent silver centres show different coordination geometries. Ag(1) is 4-coordinate, with a flattened tetrahedral geometry, and is coordinated to two cyanide groups and two nitrates. Ag(2) is 3-coordinate, and coordinated to two cyanide groups and one nitrate. One of the nitrates bridges between the silver centres.

Coordination of the cyanide groups links the $Fe_2(\mu\text{-}OMe)_2(L^1)_4$ dimers into tapes (Fig. 5a). Each cyanide group of the dimer is coordinated, and two silver centres link each dimer to its neighbour, generating 28-membered rings. The bridging nitrate interlinks these tapes into a layer structure (Fig. 5b). The layers are connected into the gross structure by short Ag···Ag contacts (3.3232(6) Å).

Selected bond lengths and bond angles for **7** are given in Table 5.

The Fe–O bond lengths range between 1.993(3) and 2.020(3) Å for the bonds to the $L^1$ ligands and from 1.947(3) to 1.977(3) Å for the bonds to the methoxides. The bite angles of the $L^1$ ligands lie

**Table 5** Selected bond lengths (Å) and angles (°) in the structure of $\{[Fe_2(\mu\text{-}OMe)_2(L^1)_4{\cdot}2AgNO_3]{\cdot}CH_3C(O)CH_3\}_\infty$ **7**[a]

| | | | |
|---|---|---|---|
| Ag(1)–N(1) | 2.311(5) | Fe(1)–O(4) | 2.017(3) |
| Ag(1)–N(2)′ | 2.251(4) | Fe(1)–O(9) | 1.977(3) |
| Ag(1)–O(14) | 2.446(5) | Fe(1)–O(10) | 1.955(3) |
| Ag(1)–O(11) | 2.564(4) | Fe(2)–O(5) | 2.017(3) |
| Ag(2)–N(3) | 2.160(4) | Fe(2)–O(6) | 2.008(3) |
| Ag(2)–N(4)′ | 2.227(4) | Fe(2)–O(7) | 2.020(3) |
| Ag(2)–O(12)″ | 2.439(4) | Fe(2)–O(8) | 2.016(3) |
| Fe(1)–O(1) | 2.008(3) | Fe(2)–O(9) | 1.976(3) |
| Fe(1)–O(2) | 1.999(3) | Fe(2)–O(10) | 1.947(3) |
| Fe(1)–O(3) | 1.993(3) | | |
| N(2)′–Ag(1)–N(1) | 136.7(2) | O(10)–Fe(1)–O(9) | 76.69(13) |
| N(1)–Ag(1)–O(14) | 87.24(19) | O(2)–Fe(1)–O(4) | 169.81(15) |
| N(2)′–Ag(1)–O(14) | 110.16(18) | O(6)–Fe(2)–O(5) | 85.02(13) |
| N(1)–Ag(1)–O(11) | 94.87(17) | O(8)–Fe(2)–O(7) | 85.07(13) |
| N(2)′–Ag(1)–O(11) | 101.71(14) | O(10)–Fe(2)–O(9) | 76.87(13) |
| O(14)–Ag(1)–O(11) | 130.44(15) | O(5)–Fe(2)–O(7) | 167.36(14) |
| N(3)–Ag(2)–N(4)′ | 141.57(16) | C(6)–N(1)–Ag(1) | 139.0(5) |
| N(3)–Ag(2)–O(12)″ | 122.79(15) | C(12)–N(2)–Ag(1)# | 155.2(4) |
| N(4)′–Ag(2)–O(12)″ | 92.84(15) | C(18)–N(3)–Ag(2) | 168.4(4) |
| O(2)–Fe(1)–O(1) | 85.08(14) | C(24)–N(4)–Ag(2)# | 155.6(4) |
| O(3)–Fe(1)–O(4) | 85.77(13) | | |

[a] Primed atoms generated by the symmetry operation $x + 1/2, -y + 1/2, z - 1/2$. Double primed atoms generated by the symmetry operation $-x + 1, -y + 1, -z$. Hashed atoms generated by the symmetry operation $x - 1/2, -y + 1/2, z + 1/2$.

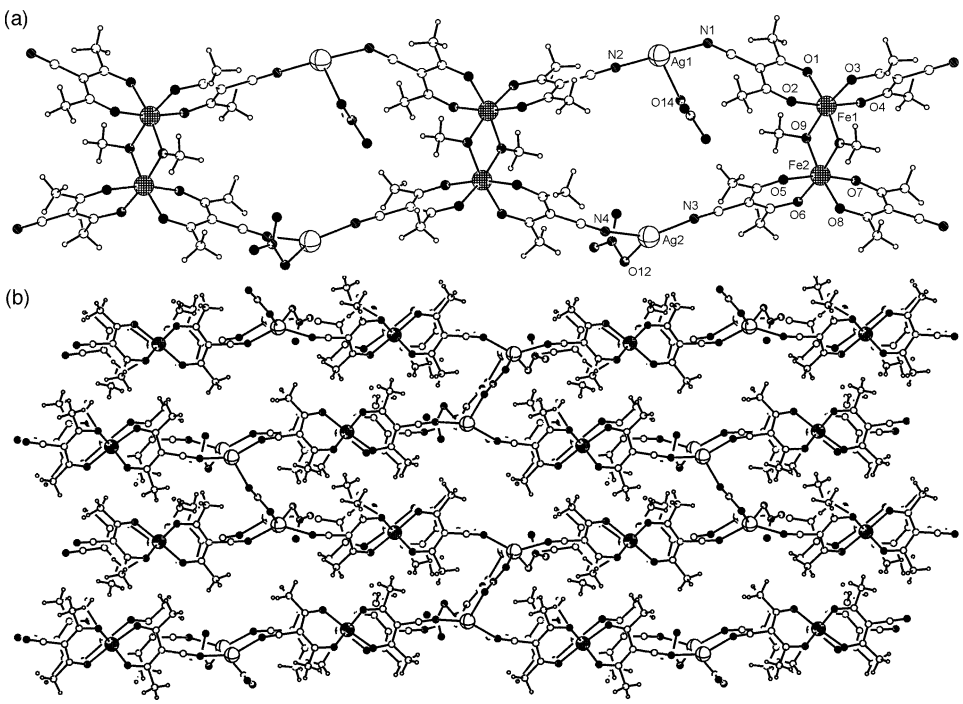


**Fig. 5** The structure of $\{[Fe_2(\mu\text{-}OMe)_2(L^1)_4{\cdot}2AgNO_3]{\cdot}CH_3C(O)CH_3\}_\infty$ **7**. Part (a) shows the tapes and part (b) shows these are interconnected by bridging nitrates to form layers. The included acetone molecule has been omitted for clarity.

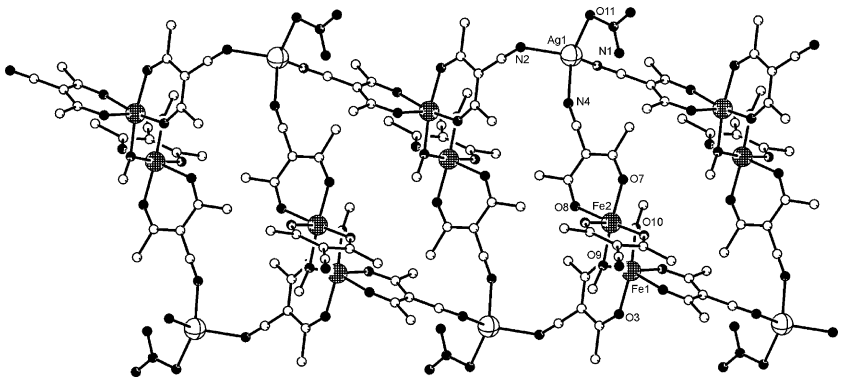


**Fig. 6** The tape structure adopted by $[Fe_2(\mu\text{-}OMe)_2(L^1)_4{\cdot}AgNO_3]_\infty$ **8**.

between 85.02(13) and 85.77(13)°. The N–Ag–N angle is 136.7(2)° for Ag(1) and 141.57(16)° for Ag(2). All of the C–N–Ag angles are distorted from linearity, ranging between 139.0(5) and 168.4(4)°. As in **3** and **6**, the $L^1$ chelate rings in **7** are not planar. The angle between the $FeO_2$ plane and the $O_2C_3$ plane defined by the ligand atoms in the chelate ring varies from 12° to 19°. These distortions are all towards the crystallographic *ac* direction and help facilitate formation of the tapes.

The asymmetric unit of $[Fe_2(\mu\text{-}OMe)_2(L^1)_4{\cdot}AgNO_3]_\infty$ **8** consists of two iron atoms, two methoxide ligands, four $L^1$ ligands, one silver centre and one nitrate anion. As in **7**, each iron centre is coordinated to two bidentate $L^1$ ligands, and bridging methoxide ligands lead to the formation of $Fe_2(\mu\text{-}OMe)_2(L^1)_4$ dimers. The silver centre adopts a distorted tetrahedral geometry with the coordination sphere occupied by three nitriles and one oxygen atom from a nitrate ion. This coordination links the $Fe_2(\mu\text{-}OMe)_2(L^1)_4$ dimers into a one-dimensional tape structure, as shown in Fig. 6. One of the nitriles on each dimer is uncoordinated, and as a consequence there are no coordination links between neighbouring tapes.

Selected bond lengths and bond angles for **8** are given in Table 6.

**Table 6** Selected bond lengths (Å) and angles (°) in the structure of $[Fe_2(\mu\text{-}OMe)_2(L^1)_4{\cdot}AgNO_3]_\infty$ **8**[a]

| | | | |
|---|---|---|---|
| Ag(1)–N(1)″ | 2.344(4) | Fe(1)–O(9) | 1.969(2) |
| Ag(1)–N(2)′ | 2.312(3) | Fe(1)–O(10) | 1.962(2) |
| Ag(1)–N(4) | 2.364(3) | Fe(2)–O(5) | 2.001(2) |
| Ag(1)–O(11) | 2.381(3) | Fe(2)–O(6) | 2.006(3) |
| Fe(1)–O(1) | 2.007(2) | Fe(2)–O(7) | 2.006(2) |
| Fe(1)–O(2) | 1.986(2) | Fe(2)–O(8) | 2.018(2) |
| Fe(1)–O(3) | 2.027(3) | Fe(2)–O(9) | 1.995(2) |
| Fe(1)–O(4) | 2.020(2) | Fe(2)–O(10) | 1.963(2) |
| N(2)′–Ag(1)–N(1)″ | 112.31(12) | O(5)–Fe(2)–O(6) | 85.51(10) |
| N(1)″–Ag(1)–N(4) | 102.92(12) | O(7)–Fe(2)–O(8) | 85.44(10) |
| N(2)′–Ag(1)–N(4) | 98.90(11) | O(10)–Fe(2)–O(9) | 77.26(10) |
| N(1)″–Ag(1)–O(11) | 116.55(12) | O(5)–Fe(2)–O(8) | 169.76(10) |
| N(2)′–Ag(1)–O(11) | 108.00(11) | Fe(1)–O(9)–Fe(2) | 101.46(10) |
| N(4)–Ag(1)–O(11) | 116.86(11) | Fe(1)–O(10)–Fe(2) | 102.87(11) |
| O(2)–Fe(1)–O(1) | 85.57(10) | C(6)–N(1)–Ag(1)″ | 134.1(3) |
| O(4)–Fe(1)–O(3) | 84.41(10) | C(12)–N(2)–Ag(1)′ | 137.4(3) |
| O(10)–Fe(1)–O(9) | 77.91(10) | C(24)–N(4)–Ag(1) | 158.4(3) |
| O(1)–Fe(1)–O(4) | 164.01(10) | | |

[a] Primed atoms generated by the symmetry operation $x + 3, -y + 2, z + 1$. Double primed atoms generated by the symmetry operation $-x + 3, -y + 2, -z$.

The Fe–O bond lengths range between 1.986(2) and 2.027(3) Å for the bonds to the $L^1$ ligands and from 1.962(2) to 1.995(2) Å for the bonds to the methoxides. The methoxide containing O(10) is symmetrically bridged, while that containing O(9) is slightly unsymmetrical. The bite angles of the $L^1$ ligands lie between 84.41(10) and 85.57(10)°. The angles around the silver centre range from 98.90(11) to 116.86(11)°. As for **6**, all of the C–N–Ag angles are distorted from linearity, with C(6)–N(1)–Ag(1)′ 134.1(3)°, C(12)–N(2)–Ag(1)′ 137.4(3)° and C(24)–N(4)–Ag(1) 158.4(3)°. The distortions from planarity of the chelate rings are lower in **8** than in the other Fe–$L^1$ compounds, with the angles between the $FeO_2$ plane and the $O_2C_3$ plane lying between 6° and 11°. C–H···N hydrogen bonds involving the uncoordinated nitrile as an acceptor link the tapes into the gross structure.

When the reaction between $Fe(L^1)_3$ and $AgNO_3$ was carried out in methanol, as opposed to an acetone–methanol mix, a different product distribution was observed. X-Ray powder diffraction measurements revealed **6** and **8** to be the major products, but small quantities of $\{[AgFe_2(\mu\text{-}OMe)_2(L^1)_4]OH{\cdot}0.4H_2O\}_\infty$ **9** were also isolated and crystallographically characterised. Although the formulae of **8** and **9** are rather similar, the network structures adopted by the compounds are completely different.

The asymmetric unit of **9** consists of half an iron atom, half a methoxide ligand, an $L^1$ ligand, a quarter of a silver atom, a quarter of a hydroxide ion and a partial occupancy water molecule. The remainder of the formula unit is generated by symmetry operations intrinsic to the space group. There is disorder in the positions of both the methoxide ligand and the hydroxide ion.

The iron centre adopts a distorted octahedral geometry, and as in **7** and **8** is coordinated to two bidentate $L^1$ ligands and two bridging methoxides giving rise to $Fe_2(\mu\text{-}OMe)_2(L^1)_4$ dimers. The bond lengths and angles within the dimer unit are similar to those observed for **8** (Table 7). The silver centre is distorted tetrahedral and coordinated to four cyanide groups. The bond angles around the silver atom lie within the range 107.1(5)–111.4(4)°, so the distortions are much lower than in the case of **7** or **8**. In addition, the C–N–Ag angle is considerably closer to linearity [C(6)–N(1)–Ag(1) 169.6(8)°] than those observed in **6**, **7** and **8**.

In contrast to the structures of **6** and **8**, and in common with **7**, all of the cyanide groups in **9** are coordinated to silver centres. In **7** this led to a sheet structure, but for **9** this gives rise to a three-dimensional network (Fig. 7a). This has the same topology as the PtS net, with the $Fe_2(\mu\text{-}OMe)_2(L^1)_4$ dimers close to being

 

**Table 7** Selected bond lengths (Å) and angles (°) in the structure of $\{[AgFe_2(\mu\text{-}OMe)_2(L^1)_4]OH{\cdot}0.4H_2O\}_\infty$ **9**

| | | | |
|---|---|---|---|
| Ag(1)–N(1)[a] | 2.210(6) | Fe(1)–O(2) | 2.016(3) |
| Fe(1)–O(1) | 2.004(3) | Fe(1)–O(3) | 1.967(3) |
| N(1)[c]–Ag(1)–N(1) | 107.1(5) | O(3)[d]–Fe(1)–O(3) | 78.1(2) |
| N(1)[b]–Ag(1)–N(1) | 110.0(4) | O(1)–Fe(1)–O(1)[e] | 167.5(2) |
| N(1)[a]–Ag(1)–N(1) | 111.4(4) | Fe(1)[d]–O(3)–Fe(1) | 101.9(2) |
| O(1)–Fe(1)–O(2) | 85.69(14) | C(6)–N(1)–Ag(1) | 169.6(8) |

Atoms generated by the following symmetry operations: *a*, $-x-2$, $y$, $-z+1/2$; *b*, $x$, $-y-2$, $-z+1/2$; *c*, $-x-2$, $-y-2$, $z$; *d*, $-x-1$, $-y-1$, $-z$; and *e* $-x-1$, $-y-1$, $z$.

square planar and the silver centre tetrahedral. There are two interpenetrating networks in the gross structure (Fig. 7b).

**Silver networks.** The reaction between $[Al(L^1)_3]$ and $AgNO_3$ in DMF–methanol was carried out in the expectation of forming an aluminium–silver coordination network. Colourless crystals were obtained from the reaction, and an X-ray crystallographic analysis revealed these to be of the compound $[Ag(L^1)]_\infty$ **10**. Selected bond lengths and bond angles for **10** are given in Table 8.

**Table 8** Selected bond lengths (Å) and angles (°) in the structure of $[Ag(L^1)]_\infty$ **10**[a]

| | | | |
|---|---|---|---|
| Ag(1)–N(1)′ | 2.156(2) | Ag(1)–O(1)″ | 2.5126(15) |
| Ag(1)–O(2) | 2.2187(16) | | |
| N(1)′–Ag(1)–O(2) | 162.10(7) | O(2)–Ag(1)–O(1)″ | 101.15(6) |
| N(1)′–Ag(1)–O(1)″ | 93.57(6) | C(6)–N(1)–Ag(1)′ | 178.1(2) |

[a] Primed atoms generated by the symmetry operation $-x, -y+1, -z+2$. Double primed atoms generated by the symmetry operation $x+1, -y+3/2, z-1/2$.

The asymmetric unit of **10** consists of a silver atom and a $L^1$ ligand. The silver adopts a distorted T-shaped coordination mode and is bound to two oxygen atoms from different $L^1$ ligands and the nitrogen atom of a cyanide group. This coordination leads to the formation of a two-dimensional sheet structure that contains both 12- and 24-membered rings (Fig. 8). In the structure, the $L^1$ ligand adopts an *anti* conformation that prevents the oxygen atoms chelating, though the two C–O bond distances are the same within experimental error. The two Ag–O bond lengths vary significantly, with the oxygen atom almost linear to the nitrogen atom forming the shorter contact [Ag(1)–O(2) 2.2187(16) Å and Ag(1)–O(1) 2.5126(15) Å].

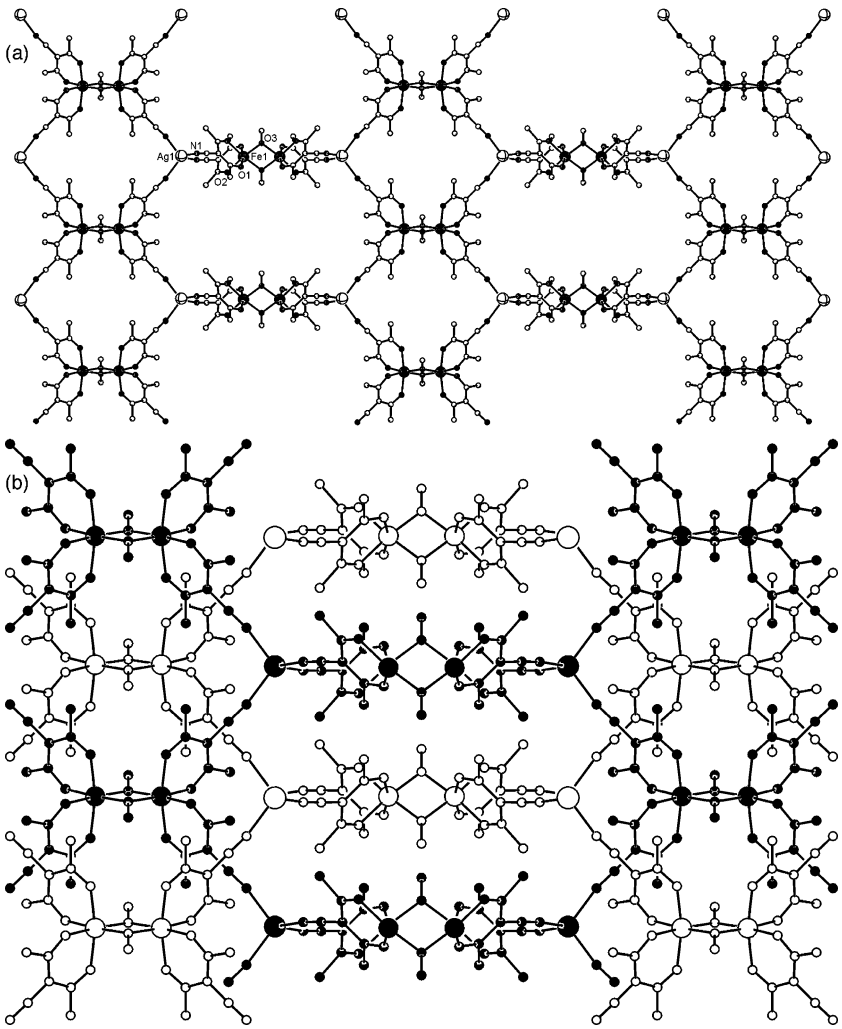


**Fig. 7** The structure of $\{[AgFe_2(\mu\text{-}OMe)_2(L^1)_4]OH{\cdot}0.4H_2O\}_\infty$ **9**. Part (a) shows one of the three-dimensional networks and part (b) shows the double interpenetration of these. The hydroxide and water molecules have been omitted for clarity.

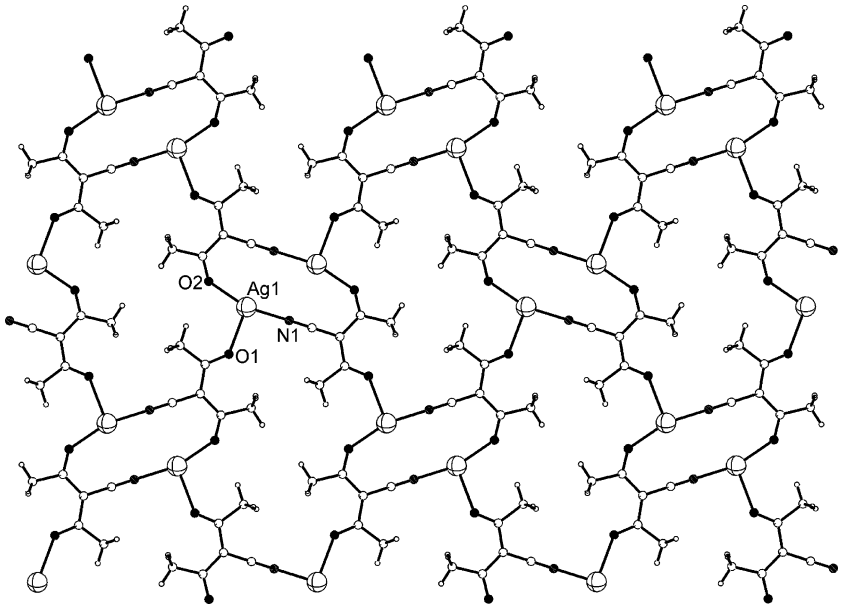


**Fig. 8** The sheet structure adopted by $[Ag(L^1)]_\infty$ **10**.

Ag···O contacts of 2.65 Å link the sheets into a three-dimensional network. The formation of $[Ag(L^1)]_\infty$ from the reaction between $Al(L^1)_3{\cdot}6H_2O$ and $AgNO_3$ illustrates the lability of $L^1$ on aluminium(III).

## Discussion

The structures of **5–9** indicate that a stepwise approach can be used successfully to form mixed-metal coordination networks based on the bifunctional ligand $L^1$. With $[Cu(L^1)_2]$, silver(I) centres connect the copper complexes into one-dimensional chains as anticipated, and these are linked into pairs through bridging nitrates. With $[Fe(L^1)_3]$, however, the observed structures were more difficult to predict, in part because not all of the cyanide groups are coordinated in the structures of **6** and **8**. Coordination of the three nitriles of $[Fe(L^1)_3]$ to three-coordinate silver(I) centres would be anticipated to lead to a two-dimensional sheet structure, analogous to that formed between $AgO_3SCF_3$ and 1,3,5-tricyanobenzene,[21] notwithstanding the deviations from regular 120° angles in $Fe(L^1)_3$ mentioned above. Non-coordination of one of the cyanide groups leads to the reduction in dimensionality observed in the structure of **6**. The products formed do not seem to depend on the stoichiometry employed in the reaction, though in the case of **6–8** this does vary the ratio of products to a small degree.

The difficulty in predicting the structures of the iron products was also compounded by the observation of $Fe_2(\mu\text{-}OMe)_2(L^1)_4$ dimers in the structures of **7**, **8** and **9**. Of these compounds, **8** forms one-dimensional chains, **7** forms two-dimensional sheets and **9** forms a three-dimensional network. $[Fe_2(\mu\text{-}OR)_2(acac)_4]$ dimers are well-established, and normally prepared from the reaction of $[Fe(acac)_3]$ with NaOR.[22] It is possible that a small degree of dissociation of $L^1$ from **3** occurs in solution, and this acts as a base for the formation of methoxide. The observation of methoxide in the structure of **2** confirms silver ions are not required to form methoxide in copper complexes of $L^1$. When samples of **3**, however, were recrystallised from methanol over a period of several weeks no reaction occurred, and powder X-ray diffraction experiments revealed the recovered solid to be pure **3**. This suggests that $Ag^+$ is necessary for dimer formation from **3**. However, the observation of dimers does suggest that the binding of $L^1$ is weaker than that of $acac^-$, and this is compounded by the observation of transmetallation in the reaction of $[Al(L^1)_3]$.

The appearance of the $Fe_2(\mu\text{-}OMe)_2(L^1)_4$ units in the structures of **7–9** suggests that these can be considered as secondary building units. There are, however, significant differences between the orientations of the cyanide groups in these dimers (Fig. 9). In **7** and **9**, the dimers form rectangular planar SBUs, with the cyanide groups almost co-planar. In contrast, the dimers in **8** form distorted tetrahedral SBUs. This difference is related to the chirality around the iron centres in the dimers. For **7** and **9**, the iron centres have opposite chirality, whereas for **8** both have the same chirality.

The dimers in **7** and **9** are rectangular planar rather than square planar, but this does not prevent **9** from forming the PtS net. In **7**, the N···N distances within each dimer range from 7.3 to 11.1 Å, whereas in **9** they are 8.8 and 10.9 Å. Surprisingly, the orientations of the rectangles differ, as in **7** the longer distances are across a single iron centre and in **9** they are across the dimer itself. This difference is due to the direction of the distortions in the chelate rings. In **7** these all occur in the same direction and this aids in the formation of the tapes. In **9** the directions of the distortions are dictated by the symmetry elements inherent in the space group.

Comparison of the calculated densities for **8** (1.733 g $cm^{-3}$) and **9** (1.317 g $cm^{-3}$) reveals that the packing in **8** is more efficient than that in **9**. The PtS network of **9** generates voids within the structure, and whilst the interpenetration reduces the size of these, it cannot completely eliminate them.

In this paper we have demonstrated that functionalised β-diketonate ligands can be used to form one-, two- and three-dimensional mixed-metal coordination networks. We are currently

 

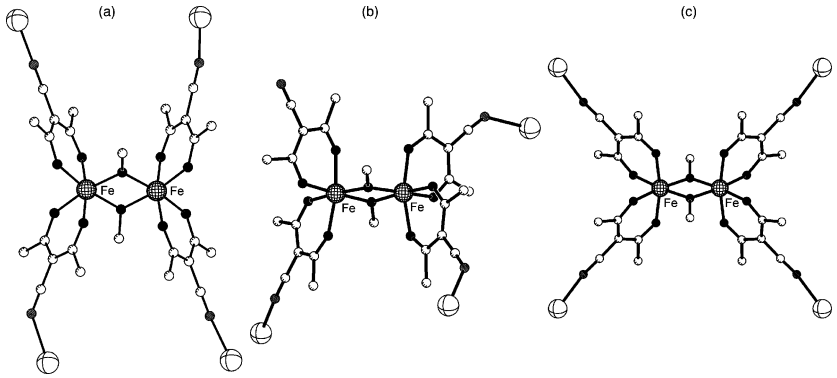


**Fig. 9** The $Fe_2(\mu\text{-}OMe)_2(L^1)_4$ dimers present in the structures of (a) **7**, (b) **8** and (c) **9**.

seeking to improve the stability of these networks by changing the linking functionality and the metal centres.

## Experimental

3-Cyano-2,4-pentanedione ($HL^1$)[18] and $[Cu(L^1)_2]$ (**1**)[20] were synthesised using the literature methods. NMR spectroscopy and microanalysis revealed water of crystallization to be present in the samples of $HL^1$, and for the reactions it was formulated as $HL^1{\cdot}0.4H_2O$. NMR spectra were recorded at 298 K on Bruker Avance 300 and 400 MHz NMR spectrometers, and referenced (for $^1H$) to residual protio solvent signals ($\delta$ 7.24 for $CDCl_3$) and to solvent resonances for $^{13}C\{^1H\}$ NMR ($\delta$ 77.2 for $CDCl_3$). Microanalysis (C, H and N) were carried out by Mr Alan Carver (University of Bath Microanalytical Service). Mass spectra were recorded by the EPSRC National Mass Spectrometry Service Centre, University of Swansea, UK. IR spectra were recorded as KBr discs on a Nicolet Protégé 460 FTIR spectrometer. Powder diffraction data were recorded on a Bruker D8 diffractometer fitted with Goebal mirrors and a 0.2 mm beam slit, and in each case, unless noted below, the experimental pattern showed a good match with that simulated from the single crystal analysis.

### Synthesis of $[Cu_6(\mu_3\text{-}OMe)_4(\mu\text{-}OMe)_2(L^1)_6]$ (2)

$Cu(NO_3)_2{\cdot}3H_2O$ (0.502 g, 2.08 mmol) and $HL^1{\cdot}0.4H_2O$ (0.521 g, 3.94 mmol) were dissolved together in methanol (40 $cm^3$). $NEt_3$ (4 $cm^3$) was placed in a sample tube which was inserted into the flask containing the methanol solution. Vapour diffusion of the base into the solution gave blue crystals of **2** after 10 h. Yield 0.352 g (82%). Anal. Calcd (Found) for $C_{42}H_{54}Cu_6O_{18}N_6$: C 38.4 (38.2); H 4.22 (4.16); N 6.40 (6.20)%. IR/$cm^{-1}$ (KBr): $\nu$(CN) at 2213s, $\nu$(CO) at 1608s (br).

### Synthesis of $[Fe(L^1)_3]$ (3)

$Fe(NO_3)_3{\cdot}9H_2O$ (0.958 g, 2.37 mmol) and $HL^1{\cdot}0.4H_2O$ (0.902 g, 6.82 mmol) were dissolved together in methanol (12 $cm^3$). $NEt_3$ (5 $cm^3$) was placed in a sample tube which was inserted into the flask. Vapour diffusion of the base into the solution gave dark-red crystals of **3** after 2 h. Yield 0.192 g (20%). Anal. Calcd (Found) for $C_{18}H_{18}FeN_3O_6$: C 50.5 (50.0); H 4.24 (4.30); N 9.81 (9.74)%. IR/$cm^{-1}$ (KBr): $\nu$(OH) at 3428m (br), $\nu$(CN) at 2208s, $\nu$(CO) at 1613s (br).

### Synthesis of $[Al(L^1)_3]{\cdot}6H_2O$ (4)

$Al(NO_3)_3{\cdot}9H_2O$ (0.120 g, 0.32 mmol) and $HL^1{\cdot}0.4H_2O$ (0.120 g, 0.91 mmol) were dissolved together in a 1 : 1 mix of methanol and water (4 $cm^3$). To this was added slowly a solution of $NaHCO_3$ (0.200 g, 2.38 mmol) in a 1 : 1 mix of methanol and water (4 $cm^3$), and the mixture stirred for 30 min. The resultant colourless solid was separated by filtration, washed with water and dried in air. Yield 0.100 g (65%). $^1H$ NMR ($CDCl_3$) $\delta$ 2.29 (s, $CH_3$), 1.55 (s, $H_2O$) $^{13}C\{^1H\}$ NMR ($CDCl_3$) $\delta$ 27.4 ($CH_3$), 92.6 (*C*CN), 118.7 (CN), 197.7 (CO). Anal. Calcd (Found) for $C_{18}H_{30}AlN_3O_{12}$: C 42.6 (43.2); H 5.92 (5.87); N 8.28 (8.47)%. IR/$cm^{-1}$ (KBr): $\nu$(CN) at 2208s, $\nu$(CO) at 1613s (br). MS (MALDI) $m/z$ 422 $[M + Na]^+$; 275 $[Al(L^1)_2 + H]^+$; 158 $[Al(L^1)]^+$, 124 $[L^1]^+$.

### Synthesis of $[Cu(L^1)_2{\cdot}AgNO_3]_\infty$ (5)

$Cu(L^1)_2$ (0.018 g, 0.058 mmol) was dissolved in DMF (2 $cm^3$) and a solution of $AgNO_3$ (0.029 g, 0.17 mmol) in methanol (2 $cm^3$) gently layered above it. Blue crystals were formed after several days at room temperature in the dark. Yield 0.014 g (50%). Anal. Calcd (Found) for $C_{12}H_{12}AgCuN_3O_7$: C 29.9 (29.8); H 2.51 (2.48); N 8.72 (8.64)%. IR/$cm^{-1}$ (KBr): $\nu$(CN) at 2211s, $\nu$(CO) at 1602s (br).

### Synthesis of $[Fe(L^1)_3{\cdot}AgNO_3]_\infty$ (6), $\{[Fe_2(\mu\text{-}OMe)_2(L^1)_4{\cdot}2AgNO_3]{\cdot}CH_3C(O)CH_3\}_\infty$ (7) and $[Fe_2(\mu\text{-}OMe)_2(L^1)_4{\cdot}AgNO_3]_\infty$ (8)

$[Fe(L^1)_3]$ (0.024 g, 0.056 mmol) was dissolved in acetone (2 $cm^3$) and a solution of $AgNO_3$ (0.029 g, 0.17 mmol) in methanol (2 $cm^3$) gently layered above it. After 2 weeks, pale red crystals had formed. X-Ray analysis (single crystal and powder) confirmed the major product in these crystals was **7** (yield 0.003 g, 10%), with **8** present as a minor product. When the solution was left for longer periods, darker red crystals precipitated from solution. These were shown by X-ray analyses to be **6** (Yield 0.009 g, 27%). Anal. Calcd (Found) for $C_{18}H_{18}AgFeN_4O_9$ (**6**): C 36.1 (35.7); H 3.03 (2.99); N 9.37 (8.97)%. IR/$cm^{-1}$ (KBr): $\nu$(CN) at 2212s, $\nu$(CO) at 1586s (br).

### Synthesis of $\{[AgFe_2(\mu\text{-}OMe)_2(L^1)_4]OH{\cdot}0.4H_2O\}_\infty$ (9)

$[Fe(L^1)_3]$ (0.024 g, 0.056 mmol) was dissolved in methanol (2 $cm^3$) and a solution of $AgNO_3$ (0.029 g, 0.17 mmol) in methanol (2 $cm^3$) gently layered above it. X-Ray powder diffraction analyses

**Table 9** Crystallographic data for compounds **2**, **3** and **5–10**

| | 2 | 3 | 5 | 6 | 7 | 8 | 9 | 10 |
|---|---|---|---|---|---|---|---|---|
| Formula | $C_{42}H_{54}Cu_6N_6O_{18}$ | $C_{18}H_{18}FeN_3O_6$ | $C_{12}H_{12}AgCuN_3O_7$ | $C_{18}H_{18}AgFeN_4O_9$ | $C_{29}H_{36}Ag_2Fe_2N_6O_{17}$ | $C_{26}H_{30}AgFe_2N_5O_{13}$ | $C_{26}H_{31.8}AgFe_2N_4O_{11.4}$ | $C_6H_6AgNO_2$ |
| $M$ | 1312.16 | 428.20 | 481.66 | 598.08 | 1068.08 | 840.12 | 802.32 | 231.99 |
| $T$/K | 150(2) | 150(2) | 150(2) | 150(2) | 150(2) | 150(2) | 173(2) | 150(2) |
| Crystal system | Triclinic | Monoclinic | Triclinic | Monoclinic | Monoclinic | Triclinic | Orthorhombic | Monoclinic |
| Space group | $P\bar{1}$ | $P2_1/c$ | $P\bar{1}$ | $P2_1/c$ | $P2_1/n$ | $P\bar{1}$ | $Pccm$ | $P2_1/c$ |
| $a$/Å | 8.6030(1) | 15.3320(2) | 7.7735(2) | 14.0460(1) | 17.2710(2) | 11.1107(5) | 7.6634(5) | 3.7884(2) |
| $b$/Å | 10.6410(2) | 13.0220(2) | 8.4210(2) | 11.3220(1) | 12.5520(2) | 11.3532(5) | 9.6825(7) | 13.4634(6) |
| $c$/Å | 14.7610(3) | 21.3520(4) | 13.4553(4) | 15.0110(1) | 18.9510(3) | 13.0922(6) | 27.1105(19) | 12.8252(6) |
| $\alpha$/° | 102.936(1) | 90 | 91.187(1) | 90 | 90 | 99.941(1) | 90 | 90 |
| $\beta$/° | 100.006(1) | 113.265(1) | 97.692(1) | 116.650(1) | 111.217(1) | 93.406(1) | 90 | 93.679(1) |
| $\gamma$/° | 104.594(1) | 90 | 117.238(1) | 90 | 90 | 96.678(1) | 90 | 90 |
| $U$/Å$^3$ | 1235.97(4) | 3916.36(11) | 772.71(4) | 2133.57(3) | 3829.83(10) | 1610.30(13) | 2011.6(2) | 652.80(5) |
| $Z$ | 1 | 8 | 2 | 4 | 4 | 2 | 2 | 4 |
| $\mu$(Mo-K$_\alpha$)/mm$^{-1}$ | 2.613 | 0.809 | 2.685 | 1.657 | 1.830 | 1.562 | 1.244 | 3.013 |
| Reflections collected | 32325 | 71520 | 9381 | 54883 | 74741 | 12013 | 13713 | 8153 |
| Independent reflections | 7172 | 11424 | 5002 | 6128 | 11179 | 6591 | 2234 | 2238 |
| $R$(int) | 0.0573 | 0.1389 | 0.0131 | 0.0415 | 0.0726 | 0.0267 | 0.0385 | 0.0279 |
| $R1$, $wR2$ [$I > 2\sigma(I)$] | 0.0387, 0.0907 | 0.0526, 0.1112 | 0.0216, 0.0564 | 0.0266, 0.0691 | 0.0587, 0.1348 | 0.0427, 0.1006 | 0.0646, 0.2246 | 0.0268, 0.0618 |
| $R$ indices (all data) | 0.0657, 0.0997 | 0.1643, 0.1460 | 0.0242, 0.0581 | 0.0305, 0.0712 | 0.1123, 0.1586 | 0.0515, 0.1063 | 0.0814, 0.2420 | 0.0354, 0.0652 |
| Largest diff. peak and hole/e Å$^{-3}$ | 0.913, −0.650 | 0.472, −0.441 | 0.496, −0.699 | 0.565, −0.752 | 1.572, −0.929 | 1.042, −1.012 | 1.190, −0.518 | 1.111, −0.727 |

revealed **6** and **8** to be to the major products, though small quantities of **9** were also isolated.

### Synthesis of $[Ag(L^1)]_\infty$ (10)

$[Al(L^1)_3]\cdot 6H_2O$ (0.023 g, 0.045 mmol) was dissolved in DMF (2 cm$^3$) and a solution of $AgNO_3$ (0.029 g, 0.17 mmol) in methanol (2 cm$^3$) gently layered above it. Colourless crystals were formed after several days at room temperature in the dark. These darken on standing, and the decomposition to metallic silver prevented satisfactory microanalysis from being obtained. Yield 0.006 g (19%, assuming all $L^1$ ligands are available).

### Crystallography

Single crystals of compounds **2**, **3**, **6** and **7** were analysed using a Nonius Kappa CCD diffractometer and Mo-K$_\alpha$ radiation ($\lambda$ = 0.71073 Å). Data for **5** and **10** were collected at Daresbury station 9.8 SMX ($\lambda$ = 0.6751 Å) while those for **8** and **9** were obtained at Daresbury station 16.2 SMX ($\lambda$ = 0.8460 Å). Details of the data collections, solutions and refinements are given in Table 9. The structures were universally solved using SHELXS-97 and refined using full-matrix least squares in SHELXL-97.[23] Multiscan absorption corrections were applied throughout and convergence was uneventful, with the following exceptions and points of note.

The asymmetric unit in **2** and **9** consists of half of a molecule, proximate to a crystallographic inversion centre. In contrast, the asymmetric unit in **3** consists of two independent molecules.

In **9**, the bridging methoxy carbon was seen to be disordered over two sites (C7A, C7B), in a 32 : 18 ratio. The solvent water and partial hydroxide also exhibited disorder over sites OS1, OH1 and OH2. Hydrogen atoms in the anion and solvent could not be reliably located and hence were omitted from the final least squares.

CCDC reference numbers 636527–636534.

For crystallographic data in CIF or other electronic format see DOI: 10.1039/b702074k

## Acknowledgements

The EPSRC is thanked for financial support. Its support for the National Mass Spectrometry Service at Swansea and the Chemical Database Service at Daresbury are also acknowledged.

## References

1 M. Eddaoudi, D. B. Moler, H. L. Li, B. L. Chen, T. M. Reineke, M. O'Keeffe and O. M. Yaghi, *Acc. Chem. Res.*, 2001, **34**, 319; S. L. James, *Chem. Soc. Rev.*, 2003, **32**, 276; C. Janiak, *Dalton Trans.*, 2003, 2781; S. Kitagawa, R. Kitaura and S. Noro, *Angew. Chem., Int. Ed.*, 2004, **43**, 2334.

2 R. Kitaura, K. Seki, G. Akiyama and S. Kitagawa, *Angew. Chem., Int. Ed.*, 2003, **42**, 428; L. Pan, K. M. Adams, H. E. Hernandez, X. T. Wang, C. Zheng, Y. Hattori and K. Kaneko, *J. Am. Chem. Soc.*, 2003, **125**, 3062; D. Bradshaw, T. J. Prior, E. J. Cussen, J. B. Claridge and M. J. Rosseinsky, *J. Am. Chem. Soc.*, 2004, **126**, 6106; S. S.-Y. Chui, S. M.-F. Lo, J. P. H. Charmant, A. G. Orpen and I. D. Williams, *Science*, 1999, **283**, 1148; G. Férey, C. Mellot-Draznieks, C. Serre, F. Millange, J. Dutour, S. Surblé and I. Margiolaki, *Science*, 2005, **309**, 2040.

3 N. L. Rosi, J. Eckert, M. Eddaoudi, D. T. Vodak, J. Kim, M. O'Keeffe and O. M. Yaghi, *Science*, 2003, **300**, 1127; J. L. C. Rowsell and

 

O. M. Yaghi, *Angew. Chem., Int. Ed.*, 2005, **44**, 4670; A. G. Wong-Foy, A. J. Matzger and O. M. Yaghi, *J. Am. Chem. Soc.*, 2006, **128**, 3494; B. Panella, M. Hirscher, H. Putter and U. Muller, *Adv. Funct. Mater.*, 2006, **16**, 520.
4 U. Mueller, M. Schubert, F. Teich, H. Puetter, K. Schierle-Arndt and J. Pastre, *J. Mater. Chem.*, 2006, **16**, 626.
5 B. Chen, C. Liang, J. Yang, D. S. Contreras, Y. L. Clancy, E. B. Lobkovsky, O. M. Yaghi and S. Dai, *Angew. Chem., Int. Ed.*, 2006, **45**, 1390; S. Bourrelly, P. L. Llewellyn, C. Serre, F. Millange, T. Loiseau and G. Férey, *J. Am. Chem. Soc.*, 2005, **127**, 13519.
6 C. D. Wu, A. Hu, L. Zhang and W. B. Lin, *J. Am. Chem. Soc.*, 2005, **127**, 8940; S. H. Cho, B. Q. Ma, S. T. Nguyen, J. T. Hupp and T. E. Albrecht-Schmitt, *Chem. Commun.*, 2006, 2563.
7 G. A. Mines, B. C. Tzeng, K. J. Stevenson, J. L. Li and J. T. Hupp, *Angew. Chem., Int. Ed.*, 2002, **41**, 154.
8 S. De. Rosa, G. Giordano, T. Granato, A. Katovic, A. Siciliano and F. Tripicchio, *J. Agric. Food Chem.*, 2005, **53**, 8306.
9 Y. B. Go, X. Q. Wang, E. V. Anokhina and A. J. Jacobson, *Inorg. Chem.*, 2005, **44**, 8265; V. R. Pedireddi and S. Varughese, *Inorg. Chem.*, 2004, **43**, 450.
10 A. D. Burrows, K. Cassar, R. M. W. Friend, M. F. Mahon, S. P. Rigby and J. E. Warren, *CrystEngComm*, 2005, **7**, 548.
11 S. Kitagawa, S. Noro and T. Nakamura, *Chem. Commun.*, 2006, 701.
12 B. D. Chandler, A. P. Coté, D. T. Cramb, J. M. Hill and G. K. H. Shimizu, *Chem. Commun.*, 2002, 1900.
13 D. L. Murphy, M. R. Malachowski, C. F. Campana and S. M. Cohen, *Chem. Commun.*, 2005, 5506.
14 P. J. Steel, *Acc. Chem. Res.*, 2005, **38**, 243.
15 S. S. Turner, D. Collison, F. E. Mabbs and M. Halliwell, *J. Chem. Soc., Dalton Trans.*, 1997, 1117; B. Chen, F. R. Fronczek and A. W. Maverick, *Inorg. Chem.*, 2004, **43**, 8209.
16 V. D. Vreshch, A. B. Lysenko, A. N. Chernega, J. A. K. Howard, H. Krautscheid, J. Sieler and K. V. Domasevitch, *Dalton Trans.*, 2004, 2899.
17 L. G. Mackay, H. L. Anderson and J. K. M. Sanders, *J. Chem. Soc., Perkin Trans. 1*, 1995, 2269.
18 C. M. Silvernail, G. Yap, R. D. Sommer, A. L. Rheingold, V. W. Day and J. A. Belot, *Polyhedron*, 2001, **20**, 3113.
19 O. Angelova, J. Macicek, M. Atanasov and G. Petrov, *Inorg. Chem.*, 1991, **30**, 1943.
20 O. Angelova, G. Petrov and J. Macicek, *Acta Crystallogr. Sect. C*, 1989, **45**, 710.
21 G. B. Gardner, D. Venkataraman, J. S. Moore and S. Lee, *Nature*, 1995, **374**, 792.
22 C. H. S. Wu, G. R. Rossman, H. B. Gray, G. S. Hammond and H. J. Schugar, *Inorg. Chem.*, 1972, **11**, 990; B. Chiari, O. Piovesana, T. Tarantelli and P. F. Zanazzi, *Inorg. Chem.*, 1984, **23**, 3398.
23 G. M. Sheldrick, *Acta Crystallogr., Sect. A*, 1990, **46**, 467; G. M. Sheldrick, *SHELXL-97, Computer Program for Crystal Structure Refinement*, University of Göttingen, Germany, 1997.